



HAL
open science

Modeling Representative Gen-IV Molten Fuel Reactivity Effects in the ZEPHYR ZPR. Part II LFR Analysis

Marat Margulis, Patrick Blaise, Erez Gilad

► To cite this version:

Marat Margulis, Patrick Blaise, Erez Gilad. Modeling Representative Gen-IV Molten Fuel Reactivity Effects in the ZEPHYR ZPR. Part II LFR Analysis. International Journal of Energy Research, 2018, 43 (2), pp.829-843. 10.1002/er.4313 . cea-02340010

HAL Id: cea-02340010

<https://cea.hal.science/cea-02340010v1>

Submitted on 17 Mar 2020

HAL is a multi-disciplinary open access archive for the deposit and dissemination of scientific research documents, whether they are published or not. The documents may come from teaching and research institutions in France or abroad, or from public or private research centers.

L'archive ouverte pluridisciplinaire **HAL**, est destinée au dépôt et à la diffusion de documents scientifiques de niveau recherche, publiés ou non, émanant des établissements d'enseignement et de recherche français ou étrangers, des laboratoires publics ou privés.

Modeling Representative Gen-IV Molten Fuel Reactivity Effects in the ZEPHYR ZPR. Part II – LFR Analysis

M. Margulis^{a,b}, P. Blaise^b and E. Gilad^{a,*}

^a *The Unit of Nuclear Engineering, Ben-Gurion University of the Negev, Beer-Sheva 84105, Israel*

^b *DEN/CAD/DER/SPESE, CEA Cadarache, CEA Cadarache, Saint-Paul-les-Durance 13108, France*

ABSTRACT

Studies related to severe core accidents are a key factor in Gen-IV safety. A novel experimental program, related to severe core accidents studies, is proposed for the future Zero-power Experimental PHYSics Reactor (ZEPHYR), to be built in Cadarache in the next decade. The innovative program aims at studying reactivity effects at high temperature during degradation of Gen-IV cores by using critical facilities and surrogate models. The current study introduces the European Lead-cooled System (ELSY) as an additional Gen-IV system into the representativity arsenal of the ZEPHYR, in addition to the sodium-cooled fast reactors. Furthermore, this study constitutes yet another step towards the ultimate goal of studying severe core accidents on a full core scale. The representation of the various systems is enabled by optimizing the plutonium content in the ZEPHYR MOX fuel. The study focuses on the representativity of reactivity variation from 900°C at nominal state to 3000°C at a degraded state in both ELSY and Advanced Sodium Technological Reactor for Industrial Demonstration (ASTRID) cores. The study utilizes the previously developed optimization sequence, which is based on the coupling of stochastic optimization process and Serpent 2 code for sensitivity analysis. Two covariance data are used, the ENDF 175-groups for ELSY and the COvariance MAtrix Cadarache (COMAC) 33-groups for ASTRID. The effect of the energy groups structure of the covariance data on the representativity process is found to be significant. The results for single degraded ELSY fuel assembly demonstrate high representativity factor (>0.95) for both the multiplication factor and the reactivity variation. It is also shown that finer energy group structure of the covariance data leads to dramatic improvement in the representativity factor of the reactivity variation.

Keywords: Representativity, Severe Accident, Core Meltdown, ZEPHYR, ASTRID, ELSY, Nuclear Reactor Safety, Nuclear Power, Energy Reliability & Sustainability, Energy Research;

* Corresponding author.

E-mail address: gilade@bgu.ac.il

1. INTRODUCTION

Safety of nuclear reactors is essential for the future prospects of nuclear energy as a reliable, affordable, and clean source of energy. Safety standards are continuously reviewed and upgraded as new research and development are performed. Continuous research, improved standards and new evaluable experiments regarding this subject are of fundamental importance for the nuclear industry. Since the Fukushima Daichii accident, there have been many analyses of its causes, consequences, and implications leading to countless new measures taken worldwide by the nuclear community [1 2]. These measures include the reassessment of current and future designs of nuclear power plans (as well as research reactors and critical facilities) against extreme accidental conditions.

Although severe core accidents (SCA) are always in the spotlight during the design process of nuclear systems, especially after TMI-2 and Chernobyl, came the Fukushima Daichii accident in 2011 and showed that there are yet many factors that are not considered [3 4]. Adequate analyses are needed for all phases of severe accident's progression in order to improve the safety margins of the design. The main gaps that require further research are identified by the EUROSAFE forum [5]. These include problems related mainly to mechanical, chemical, and material problems, which are all related to the reactor's behavior during an SCA.

When considering SCA in Gen-IV future systems [6], such as Sodium-cooled Fast Reactors (SFRs) and Lead-cooled Fast Reactors (LFRs), the SCA progression is strongly coupled to the neutronic behavior of the core. This feature, which constitutes a major difference from Light Water Reactors (LWRs), results from the fact that fast core configurations (i.e., material balance and geometry) do not create the most reactive configuration. Therefore, changes to the core layout, i.e., material relocation in the core due to SCA (e.g., fuel, coolant, structural materials), can potentially lead to positive reactivity insertion and unrestrained power excursion. Therefore, a detailed study of SCA progression is required to estimate the neutronic characteristics of the core during different stages of SCA [7].

Most of the neutronics R&D related to SCA studies is based on best-estimate computational tools, as it is impractical to compromise a nuclear reactor integrity for experimental analysis of extreme conditions. For that reason, the support of analytical research by an experimental program for the core's neutronics behavior during SCA is of utmost importance for the continued qualification of best-estimate computational tools and monitoring instrumentation.

The progression of SCA in a nuclear reactor is a non-linear step-wise process, which can develop in a wide range of directions with a large number of associated degraded configurations.

1
2
3 Moreover, the SCA progression timescale is extremely slow with respect to the neutronics time
4 scale. Hence, the study of neutronics behavior during SCA can be performed utilizing a
5 quasi-static approach, at least to validate instantaneous configurations during the meltdown
6 process. This can be attained by validating computational results versus *relevant* experimental
7 data gathered in a critical facility. The importance of “representative” experimental programs
8 emerges from this crucial need to transfer (or “translate”) experimental data, measured in a
9 (zero-power) critical facility, to the equivalent information in the reference power system. Hence,
10 “Best-Representative” experiments is a key factor in the safety design of nuclear systems
11 (current and future).
12

13
14 By ensuring high representation of numerous integral parameters, e.g., criticality or reactivity
15 variations, it is possible to provide a “Best-Estimate” neutronic analysis of an investigated
16 system in a safe and controlled environment of a Zero-Power Reactor (ZPR) [7 8 9]. Essentially,
17 representative experiments provide information on physical (neutronic) quantities of the
18 investigated power system, e.g., criticality, reactivity changes, flux distribution, spectrum,
19 reactivity feedbacks, by appropriate experimental measurements and analysis in a mock-up
20 system.
21

22
23 Previous studies showed that best representative SCA configurations (i.e., with high
24 representativity factor) can be achieved on a single SFR fuel assembly level [7].
25

26
27 The previous work [7] focused on the Advanced Sodium Technological Reactor for Industrial
28 Demonstration (ASTRID) reduced void fraction (CFV) core [10]. Recent developments related
29 to the ASTRID project experienced substantial modifications [11], with a significant reduction
30 in power (from 600 MWe to 100-200 MWe). Nevertheless, the ASTRID CFV concept presents
31 an interesting challenge in terms of severe accidents studies, due to the high heterogeneity of the
32 core. In light of these recent developments, the Commissariat à l'énergie atomique et aux
33 énergies alternatives (CEA) decided to expand the scope of its severe accidents studies beyond
34 ASTRID-like SFRs designs. This step is supposed to assist in ensuring the high scientific and
35 industrial attractiveness of the future Zero-power Experimental PHYSics Reactor (ZEPHYR)
36 facility [12]. This paper describes the extension of the ZEPHYR representativity capabilities
37 beyond the ASTRID-like core to include the European Lead-cooled SYstem (ELSY) [13] on a
38 single fuel assembly level.
39

40
41 The extension of the representativity capabilities of the ZEPHYR reactor is facilitated, to a large
42 extent, by the unique nuclear fuel stockpile of the MASURCA reactor, available at CEA research
43 center at Cadarache. This stockpile contains a wide variety of fuel materials (MOX, enriched
44
45
46
47
48
49
50

UO₂, metallic uranium, and plutonium, etc.) in different geometries (pins, plates, bars, slabs) and representative coolant bars (sodium and lead). The availability of this fuel stockpile provides a high degree of flexibility in the design of an experimental ZEPHYR core. This is a significant advantage to the proposed experimental program thanks to the possibility that high representative core configuration can be designed and built using the existing fuel stockpile without the need for additional new fuel manufacturing.

In section 2, the methodology developed for designing best-representative experiments is detailed, and a short overview of the ZEPHYR project is presented, as well as a description of the two Gen-IV reference systems (ASTRID and ELSY) considered in this study. In section 3, the results of best-representative experiment design for a single ELSY LFR fuel assembly are described and discussed, and the representativity of a single ASTRID SFR fuel assembly is revisited. Conclusions and discussion are presented in section 4.

This study is the result of a scientific collaboration between CEA Cadarache and the Unit of Nuclear Engineering at Ben-Gurion University of the Negev.

2. METHODOLOGY AND EXAMINED SYSTEMS

In this section, the methodology developed and implemented for designing best-representative core configurations is described. Also, the mathematical model of the representativity process is summarized and the Gen-IV nuclear systems under investigation are described, i.e., ZEPHYR, ASTRID-CFV, and ELSY.

2.1. Representativity method

The representativity model is based on a method proposed in [14]. The importance of best-representative experiment design stems from its capability to transfer (or “translate”) experimental data, measured in a mock-up facility, to the equivalent information in the reference power system. This is of great potential for supporting the design of future systems, e.g., the Molten Salt Reactor experiments recently launched at Petten, Netherlands [15].

The underlying hypothesis of the method relies on the similarity comparison of the sensitivity profiles of the integral quantity under investigation. The similarity is quantified by the definition of the representativity coefficient (r_{RE}), as presented in Eq. (1).

$$r_{RE} = \frac{S_R^t V S_E}{\sqrt{S_R^t V S_R} \sqrt{S_E^t V S_E}} \equiv \frac{S_R^t V S_E}{\epsilon_R \epsilon_E}, \quad (1)$$

where the subscripts E and R correspond to the experimental mock-up and reference power systems, respectively, S is the sensitivity vector (response) of the integral quantity to Nuclear Data (ND) in the two systems, and V is the variance-covariance matrix between ND. The numerator in Eq. (1) represents the covariance between the experimental mock-up and the reference power system responses, while the terms in the denominator, i.e., $S_R^t V S_R$ and $S_E^t V S_E$, represent, respectively, the priori variance (uncertainty) of the relevant quantity in systems E and R due to ND uncertainties, propagated by the classical sandwich rule [16]. The more the reference sensitivity (S_R) is similar to the experimental sensitivity (S_E), the closer the representativity factor (r_{RE}) is to unity. A representativity factor close to unity indicates that the two systems are highly correlated in terms of neutronic sensitivities (of the relevant quantity) with respect to the covariance data V .

In the previous analysis [7], the COvariance MATrix Cadarche V01 (COMAC-V01) and the JEFF-3.1.1 nuclear data evaluation were utilized in the representativity process. However, the COMAC-V01 does not contain information on lead. Therefore, the ENDF/B-VII.1 nuclear data evaluation was utilized together with the publicly available covariance matrix, which can be obtained from the Nuclear Energy Agency (NEA) Java-based Nuclear Data Information System (JANIS) [17]. The sensitivity vectors were calculated using the Serpent v2.29 Monte Carlo code [18].

The application of the representativity method for the design of an experimental system enables the prediction of *a posteriori* reduction factor in the reactor response uncertainty (ϵ_R^*) once the experimental information is assimilated. The reduction factor is given by

$$(\epsilon_R^*)^2 = (\epsilon_R)^2(1 - \omega r_{RE}^2), \quad (2)$$

where $\omega = (1 + \delta E^2 / \epsilon_E^2)^{-1}$ is called “experimental weight” factor, or an “experimental importance”, and δE is the experimental uncertainty. This factor represents the amount of transferable precision of the integral physical quantity versus its propagated uncertainty from ND. Within the limit of $r_{RE} = 1$ and the ratio $\delta E^2 / \epsilon_E^2 \rightarrow 0$, the reduction factor $\epsilon_R^* / \epsilon_R$ vanishes. However, this is not the case as shown in what follows. The C/E bias from the experimental parameter can be transpositioned to the target parameter bias $\hat{R} - R_0$ (posteriori and priori calculated values) can be written as follows -

$$\frac{\hat{R} - R_0}{R_0} = \alpha \left(\frac{E - C}{C} \right), \quad (3)$$

where the transposition factor α is expressed as [19]

$$\alpha = \frac{S_R^t V S_E}{\delta E^2 + \epsilon_E^2} = \omega r_{RE} \frac{\epsilon_R}{\epsilon_E} . \quad (4)$$

2.2. The ASTRID CFV-V0 core

The ASTRID concept was proposed to answer the requirements for safety, sustainability, economy, and non-proliferation goals, which were set by the Gen-IV forum [6]. The selection of an SFR system for the ASTRID project was based, to a large extent, on the extensive and invaluable experience of the French nuclear industry with the PHENIX and SUPERPHENIX SFR systems. In recent years, several core layouts were proposed for the ASTRID core [20]. A most promising concept was found to be the reduced void fraction (CFV) core, where the core is arranged in a hexagonal lattice and consists of four axial regions: the lower blanket, the lower fissile zone, the intermediate blanket, and the upper fissile zone, as described in Figure 1. The main parameters of the CFV-V0 are summarized in Table 1.

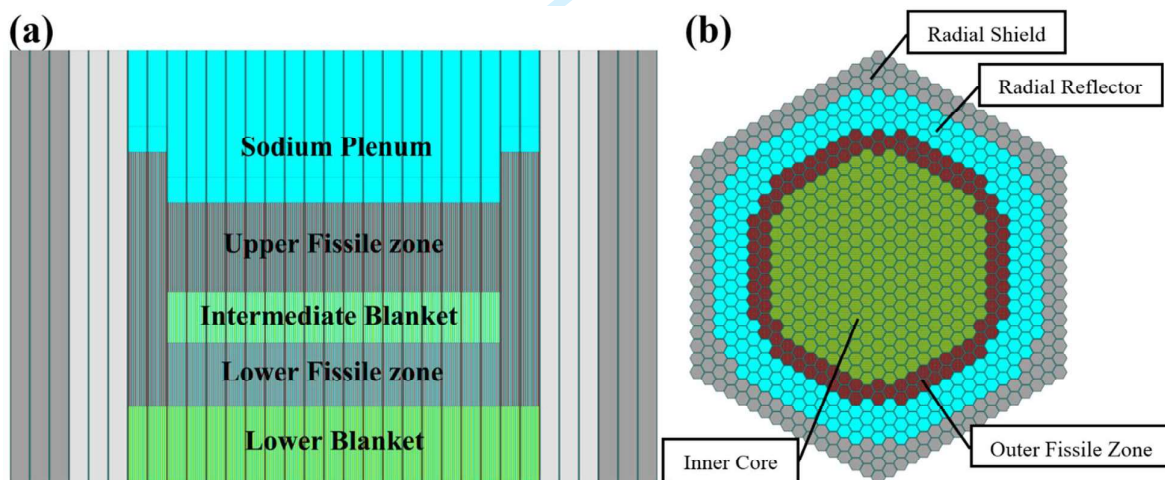


Figure 1. ASTRID CFV-V0 core layout: (a) axial cut (b) radial cut.

Table 1: Design parameters for the CFV-V0 core [10]

Core Design Parameter	CFV-V0
Nominal thermal power [MWth]	1500
Primary coolant	Sodium
Inner core dimensions	
- Lower blanket height [cm]	30

- Lower fissile zone height [cm]	25
- Intermediate blanket height [cm]	20
- Upper fissile zone height [cm]	35
- Inner core radius [cm]	133
- Assembly pitch [cm]	17.5
Outer fissile zone dimensions	
- Lower blanket height [cm]	30
- Fissile zone height [cm]	100
- Outer fissile zone radius [cm]	163
- Assembly pitch [cm]	17.5
Fissile zones PuO ₂ enrichment (inner/outer) [%]	23/23
Effective delayed neutron fraction (β_{eff}) [pcm]	364
100% void reactivity worth at equilibrium [\$]	-1.2

2.3. European Lead-cooled System - ELSY

Similar to the SFR, Lead-cooled Fast Reactor (LFR) is also one of the six fast systems selected by the Gen-IV forum as best candidates to comply with the future requirements of the nuclear industry. LFRs present some advantages in terms of safety in unprotected severe accidents, mainly thanks to the high boiling temperature of lead (about 1750°C) with respect to SFRs (sodium boiling temperature about 883°C). However, lead as a coolant is not free of faults. The main challenge in lead-cooled systems is the erosion of protective oxide layers, leading to enforcing an upper limit on coolant velocity (around 2.5-3 m/s) [21]. This limitation practically reduces the heat removal capability of the lead with respect to sodium (typical sodium flow velocity is around 10 m/s). As a result, the pin-wise pitch in LFR is larger than in SFR, resulting in better fluid circulation and enhanced safety performances. Corrosion of structural materials is also a major concern in future LFR systems. One possible way to overcome the corrosion problem is through controlling the oxygen content in the lead. Such technology was used in the Russian Alpha-class submarines, which was effective at temperatures up to 820°K [22].

Considering the two systems, LFRs presents safety-related advantages during unprotected severe accidents, mainly due to a better natural circulation and the higher boiling temperature. However, the corrosion of structural materials can lead to blockages of flowing channels, which can be followed by complete channel voiding. Moreover, the experience with LFR is very limited (mainly in the Russian Alpha-class submarines) and public information is unavailable. Therefore, these systems must go through further investigation before construction, making the ZEPHYR facility an excellent candidate to serve as an experimental mock-up.

Several LFR concepts are currently under investigation worldwide. The accelerator-driven system Multi-purpose hYbrid Research Reactor for High-tech Applications (MYRRHA) in SCK Belgium [23], the BREST-300 and BREST-1200 in Russia [24], the Advanced Lead-cooled Fast Reactor European Demonstrator (ALFRED) [25], and the European Lead SYstem (ELSY) [26] in Italy.

While the previous study focused on ASTRID SFR system, the current study focuses on the ELSY LFR system, which provides accessible information regarding geometry, material balance, and operational conditions [27]. The core layout of ELSY is shown in Figure 2, and the main characteristics are summarized in Table 2. The active core region of ELSY and the ASTRID is similar (about 120 cm), and the two systems share the same thermal power level (1500 MWth). However, the ASTRID core is much more compact due to its axial heterogeneity, which requires higher PuO₂ content in its MOX fuel. Furthermore, the ELSY core diameter is larger than that of the ASTRID core.

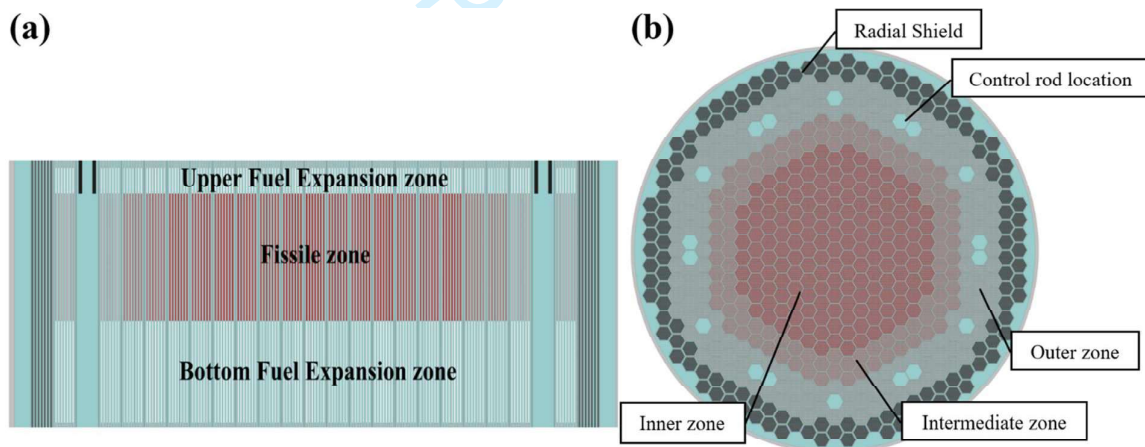


Figure 2. ELSY core layout: (a) axial cut (b) radial cut.

Table 2: Design parameters for the ELSY core [26 27]

Core Design Parameter	ELSY
Nominal thermal power [MWth]	1500
Primary Coolant	Lead
Core dimensions	
- Lower fuel expansion zone [cm]	96
- Fissile zone [cm]	120
- Upper fuel expansion zone [cm]	24
- Core radius [cm]	290
Fissile zones PuO ₂ enrichment (inner/intermediate/outer) [%]	14.5/15.5/18.5

Considering SCA in ELSY, two configurations are considered as extremes. The first configuration consists of a full blockage of a coolant channel and meltdown of the fuel, followed by stratification of materials, i.e., fuel on the bottom and structural materials on top, with a void above. The second configuration is similar to the first one with a single difference, i.e., the presence of lead on top of the melted zone. The different degraded configurations are shown in Figure 3.

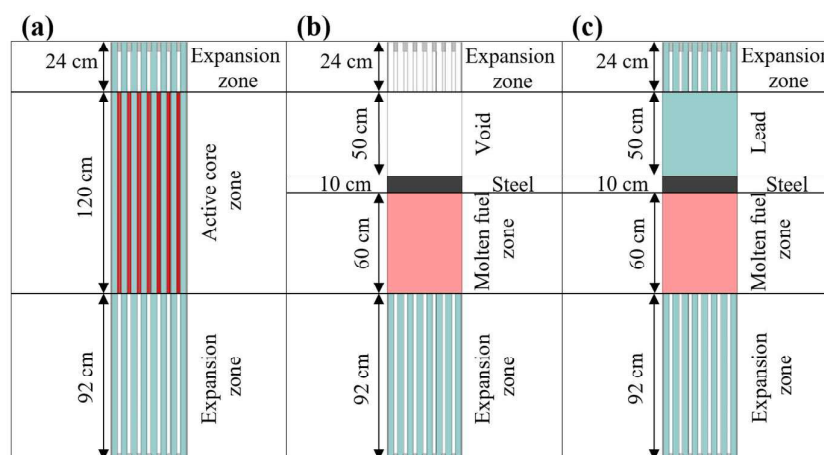


Figure 3. Degraded configuration considered in ELSY SCA studies. (a) reference intact ELSY fuel assembly (b) molten ELSY fuel zone with a void on top (c) reflooded molten pool.

3. RESULTS AND DISCUSSIONS

This section deals with the design of a representative experimental program in a ZPR related to neutronic effects during severe core accidents in Gen-IV reactors. First, uncertainty propagation of the ELSY reactor is presented, followed by a short summary of the ASTRID uncertainty analysis. Second, the methodology previously developed for the optimal design of the experimental program on a single fuel assembly level [7] is executed with respect to a single ELSY fuel assembly degraded states (Figure 3). Finally, based on the lessons learned from the study on a single ELSY fuel assembly, the representativity of a single degraded ASTRID fuel assembly is revisited.

3.1. Uncertainty propagation in the ELSY design

The uncertainty propagation enables a better understanding of the neutronic characteristics of the

reactor under investigation. For the ELSY design, the uncertainty propagation is performed using the ENDF/B-VII.1 nuclear data evaluation, in 175 energy groups. The utilization of additional nuclear data library with a fine energy mesh (175 groups for ENDF vs. 33 groups for JEFF-3.1.1) provides further verification of the models' flexibility in the design of the experimental program.

The results of the uncertainty propagation on the multiplication factor are summarized in Figure 4 and Table 3. The results indicate that there are *six* major isotopes that contribute to the total propagated uncertainties, i.e., ^{56}Fe , $^{206,207}\text{Pb}$, ^{238}U , and $^{239,240}\text{Pu}$. The propagation of uncertainties, performed with the ENDF covariance data, follows the same trend obtained with the JEFF covariance data evaluation [28 29], similarly to previous analysis of experimental programs related to SCA studies (the SNEAK-12A/B experimental program [30 31]). The uncertainty related to ^{238}U and ^{239}Pu remains high in the two different evaluations. Furthermore, the total propagated uncertainty related to ND remains at a magnitude of ~ 1000 pcm, which is similar to the uncertainty estimation performed for the ASTRID core (section 3.2).

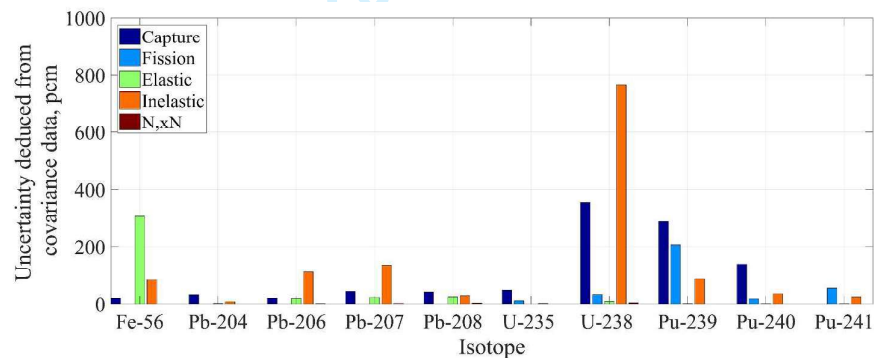


Figure 4: Propagated uncertainties for the ELSY core with ENDF/B-VII.1 covariance data [17].

Table 3: Breakdown of total propagated uncertainties for ELSY core [pcm]

Isotope	Capture	Elastic scattering	Fission	Inelastic scattering	N,xN	Total
^{56}Fe	20.2	305.2	0.0	83.6	0.0	317.1
^{204}Pb	31.5	1.6	0.0	8.1	0.1	32.6
^{206}Pb	21.0	19.4	0.0	110.6	1.1	114.2
^{207}Pb	43.3	23.0	0.0	135.3	1.9	143.9
^{208}Pb	40.8	24.8	0.0	29.0	3.1	55.9
^{235}U	47.6	0.1	11.0	1.8	0.0	48.9
^{238}U	355.8	9.2	32.1	766.0	4.1	845.3
^{239}Pu	287.5	1.0	207.3	86.5	0.3	364.9

^{240}Pu	138.7	0.6	18.5	35.4	0.1	144.3
^{241}Pu	0.0	0.6	54.5	24.1	0.3	59.6
Total	486.0	307.8	217.8	796.6	5.6	1006.4

The uncertainty propagation analysis (Table 3) reveals interesting behavior regarding individual isotopes' contribution to the propagated uncertainties. The isotopic composition used in ELSY is of natural lead, where the isotopic breakdown is

Isotope	^{204}Pb	^{206}Pb	^{207}Pb	^{208}Pb
Abundance	1.4%	24.1%	22.1%	52.4%

The uncertainties associated with the inelastic scattering show that although ^{208}Pb is the most abundant isotope, it does not exhibit the highest propagated uncertainty. Moreover, its propagated uncertainty is not much higher than the uncertainty related to ^{204}Pb . Furthermore, the propagated uncertainty for inelastic scattering is much lower for ^{208}Pb than for $^{206,207}\text{Pb}$. This behavior is associated with the inelastic scattering cross-section of the lead isotopes, as shown in Figure 5, which is a threshold reaction. The above behavior results from the difference in the energy thresholds for the different isotopes, with the ^{204}Pb threshold being the highest with respect to the other isotopes. Moreover, the uncertainties associated with inelastic scattering cross-section of ^{208}Pb are substantially lower with respect to the other isotopes.

Thus, the impact of the different lead isotopes on the propagated uncertainties of the ELSY design exhibit complex behavior, which depends not only on the isotopic abundance but on the nuclear data as well.

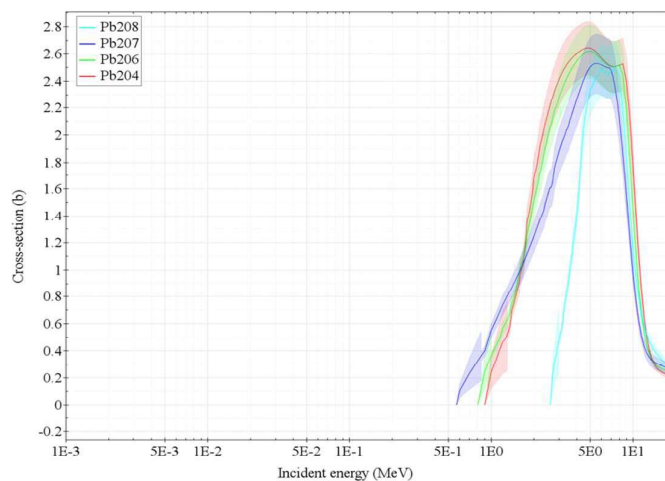


Figure 5. Inelastic scattering cross section for the different lead isotopes from ENDF/B-VII.1 evaluation.

3.2. Uncertainty propagation in the ASTRID design

The main contributors to the total uncertainty of the ASTRID core are the heavy isotopes ^{238}U and $^{239,240}\text{Pu}$ (Figure 6). The total propagated uncertainty in the ASTRID core reaches 1400 pcm, which is slightly higher than that of the ELSY core. The main difference (with respect to the ELSY core) are observed in the capture of ^{238}U and fission of $^{239,240}\text{Pu}$, attributed to their reduced uncertainties in ENDF in comparison to COMAC-V01 (Appendix A).

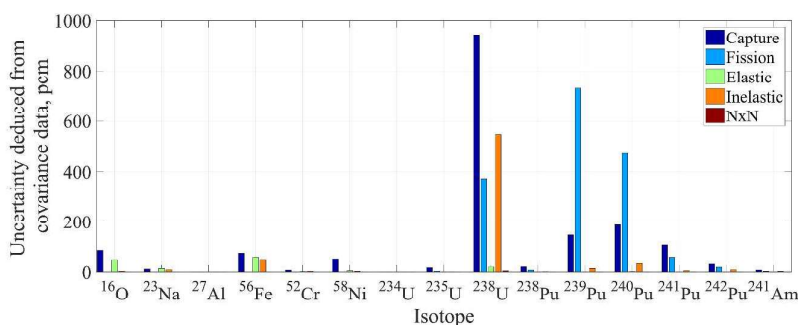


Figure 6: Propagated uncertainties for the ASTRID CFV-V0 core with COMAC-V01 [7].

Thus, the isotopes considered for representativity in the two systems are similar, i.e., ^{238}U , $^{239,240,241}\text{Pu}$, and ^{56}Fe . Therefore, the only difference between the two systems in terms of representativity calculations, is the coolant type, i.e., ^{23}Na for ASTRID and $^{204,206,207,208}\text{Pb}$ for ELSY.

At this point of the study, it is reasonable to assume that it is possible to design high representativity experimental ZEPHYR configuration for high-temperature reactivity variations in an ELSY fuel assembly. This argument is supported by the great similarity between the propagated uncertainties in the two Gen-IV systems, the ELSY and the ASTRID, and by the fact that high representativity was already obtained for high-temperature reactivity variations in an ASTRID fuel assembly. The highly representative experimental ZEPHYR configurations would be achieved by identifying the relationship between temperature effects in ELSY and density effects in ZEPHYR.

3.3. Representativity of a single degraded ELSY fuel assembly

The results presented in this section are obtained utilizing the same optimization methodology

that was presented for the ASTRID assembly degradation in a previous study [7]. The study is concentrated on the temperature variation from 900°C at the nominal state to 3000°C at the degraded configuration of the ELSY fuel assembly. The optimization methodology is based on the Particle Swarm Optimization (PSO) [32], for the maximization of the representativity factor through the search for the “perfect fuel” that will ensure the highest r_{RE} value.

The term “perfect fuel” refers to a hypothetical representative ZEPHYR fuel assembly with such plutonium oxide content that provides the highest representativity of the power system. The optimal plutonium content is a degree of freedom of the optimization process and theoretically can assume any value between 0-100%. This is in contrast to, e.g., the “MASURCA fuel”, which is an existing fuel repository of the MASURCA fast critical assembly and is comprised of fuel element of different geometries and different plutonium contents.

The examined configurations that would be loaded into the ZEPHYR facility are shown in Figure 7. The reference fuel assembly for the representativity studies (Figure 7a) is a square type lattice that is loaded with 8 lead rodlets, 2 natural UO_2 pins, and 6 MOX pins. This type of fuel assembly was found to be the most representative of the ELSY undegraded fuel assembly and is thus loaded into the ZEPHYR core. Consequently, the multiplication factor representativity of a single fuel ELSY assembly reaches a value of 0.96. The two degraded configurations that are considered are a meltdown of the MOX fuel and the formation of a molten region with material stratification, without and with lead reflooding of the voided zone above the melted fuel (Figures 7b and 7c, respectively).

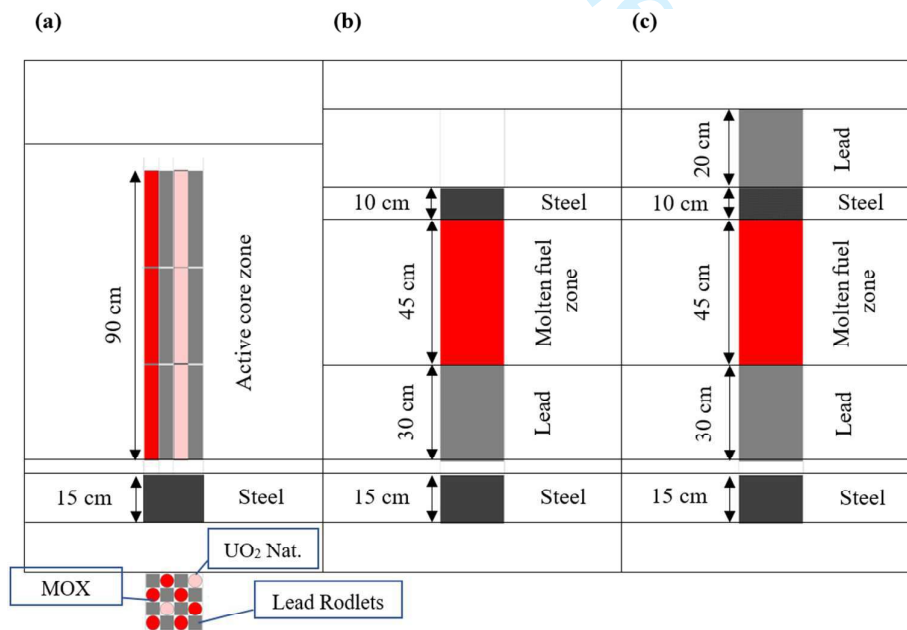


Figure 7: Fuel assembly configuration for representativity studies of ELSY SCA to be loaded into ZEPHYR. (a) reference (b) degraded configuration 1: void above melt (c) degraded configuration 2: lead above melt.

In the previous study of a single ASTRID fuel assembly [7], a variety of temperatures were considered (20°C and 900°C for the nominal state, 20°C, 1000°C, 2000°C and 3000°C for the degraded configuration) for research purposes. In this study, only realistic conditions are examined, i.e., temperatures of 900°C for normal core operation conditions and of 3000°C for degraded configurations. The results of the PSO calculations are summarized in Figure 8 and Table 4. The results show that in the case of the LFR core, the representativity exhibits a distinct behavior as a function of plutonium content. Unlike in the SFR single degraded zone simulations, where only a single point gives representativity value above 0.85, in the LFR case, a wide range of plutonium content exist (below 20%) with representativity values above the required value of 0.85. Around 25% PuO₂ content the representativity drops sharply, and as the content of the PuO₂ is further increased, the representativity monotonically increases towards an asymptotic value of around $r_{RE} = 0.6$.

The comparison of the sensitivity profiles of the reactivity variations (Figure 9) in the ZEPHYR vs. the ELSY systems shows that the sensitivity profiles are very similar, especially, for the capture in ²³⁸U and fission of ²³⁹Pu, which are the dominant reactions in both systems.

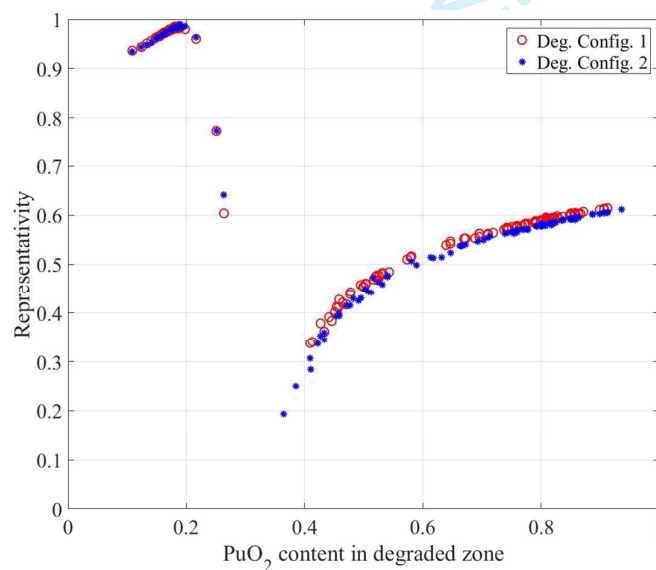


Figure 8: PSO results for the representativity of a single degraded ELSY fuel assembly.

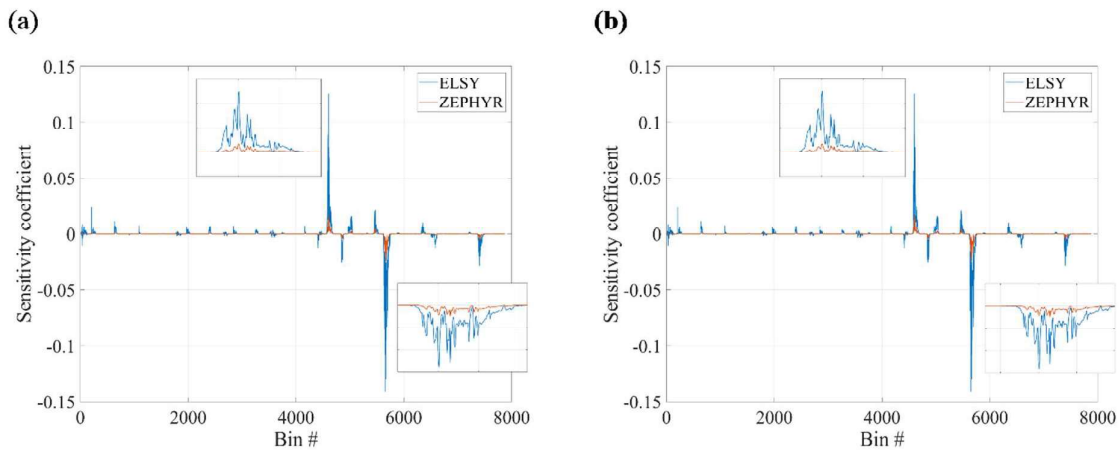


Figure 9: Sensitivity profiles of the reactivity variations in the ZEPHYR and ELSY. (a) ref. vs. deg. config. 1 (b) ref. vs. deg. config. 2. The insets show “zoom-in” on the large peaks.

Table 4: Representativity of reactivity variations for the different degraded ELSY configuration and the optimal plutonium content in the ZEPHYR fuel.

Core	Degraded configuration	PuO ₂ content in MOX	r_{RE}
ELSY (ENDF/B-VII.1)	Ref. to deg. config. 1	19.8%	0.96
	Ref. to deg. config. 2	18.8%	0.96

3.4. Revisiting the representativity of a single degraded ASTRID fuel assembly

In light of the excellent results for the single ELSY fuel assembly degradation representation, a revisit of the results obtained for the single ASTRID fuel assembly degradation is performed, mainly in order to estimate the impact of different nuclear data library and finer structure of energy groups (COMAC – 33-groups, ENDF – 175-groups) on the representativity process.

Previous results, obtained using JEFF-3.1.1 and COMAC [7], show that the target representativity factor of 0.85 can be obtained just for a very narrow range of PuO₂ content values. However, a change in both the nuclear evaluated data set and the associated covariance matrix can substantially alter the results. For example, changing only the covariance matrix from COMAC to Updated COvariance Matrix (UCOM) [33] increase the required PuO₂ content without changing the maximal representativity factor of 0.85 [7]. The increase in PuO₂ content, in this case, is due to the increased importance of ²⁴⁰Pu in the representativity process. Utilizing the ENDF and its associated covariance data with finer energy mesh (175g vs 33g) leads to increase in representativity (0.91), probably because less information is lost during down-scaling (coarse-meshing) of the covariance matrix. Both revisited ASTRID and ZEPHYR configurations are shown in Figure 10, and the results of the representativity analysis are summarized in Table

5.

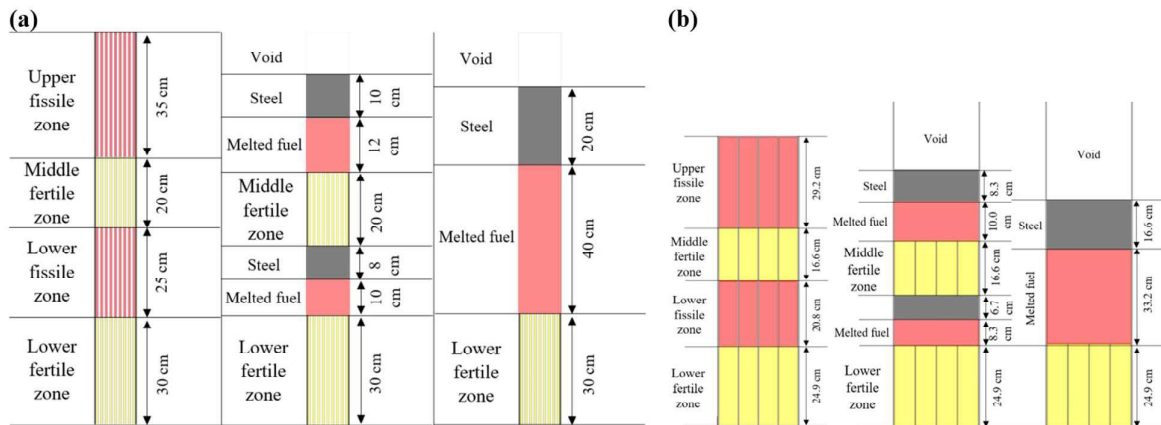


Figure 10: Revisited degraded configurations of a single ASTRID fuel assembly [7], from voided fuel assembly to a single molten zone (Note: the figures are not on the same scale). (a) ASTRID configurations (b) ZEPHYR configurations.

In the previous analysis, it was demonstrated that the representativity results are strongly linked to the uncertainty level [7]. For example, when the uncertainties were reduced for key isotopes and reactions (i.e., ^{238}U and ^{239}Pu), the representativity level dropped. This is due to the increase in the relative importance of other isotopes in the representativity process, which may behave differently in the experimental system.

In this study, three main reactions govern the representativity process in all examined systems, i.e., capture and inelastic scattering of ^{238}U and fission of ^{239}Pu . The covariance data from COMAC-V01 in 33-groups and from ENDF in 175-groups are shown in Figures A1, A2, and A3 in the Appendix.

Noticeable differences in the uncertainty vectors of all the presented reactions are observed. The uncertainties associated with ENDF covariance data are notably lower with respect to the COMAC-V01 data. The impact of the uncertainty reduction of the representativity process was previously examined by reducing the uncertainties in COMAC and the generation of UCOM [33]. This change led to the increase in the required amount of PuO_2 in the degraded MOX zone in order to achieve the required level of representativity (Table 5). The change in the PuO_2 content stems from the different plutonium vectors associated with the ASTRID and with the ZEPHYR, where the latter contains much less ^{240}Pu . Hence, the weight of ^{240}Pu in the representativity process is drastically increased due to the reduction in the uncertainties in ^{238}U and ^{239}Pu .

16 / 23

Table 5: Plutonium vectors

System	^{238}Pu	^{239}Pu	^{240}Pu	^{241}Pu	^{242}Pu	^{241}Am
ASTRID [34 35]	3%	55%	26%	7%	7.5%	1.5%
ELSY [26 27]	2.3%	57%	27%	6.1%	7.6%	-
ZEPHYR	0.8%	70%	18%	8%	2%	0.2%

Although JEFF and ENDF are two separate evaluations, the data collapsing to energy groups leads to a change in the shape of the correlation matrix. The correlation between the different energy groups (off-diagonal terms) is smoothed out in the 33g with respect to the 175g. This is despite the fact that the collapse of the covariance matrix to a small number of energy groups conserves the propagated uncertainty [36]. In the case of the representativity process, this energy group collapse may have a profound impact on the value of r_{RE} , as in the current study, since some information is inevitably being lost during the collapsing process.

The impact on the search space shape due to the change in the covariance data is also significant, as shown in Figure 11. The overall behavior is similar to the previous findings, with three zones, i.e., the relatively low representativity values at high PuO_2 contents, a "death valley" cut-off, and the high representativity region. However, when using the previous 33g covariance data, the high representativity region is represented by a single point, whereas in the current case (of 175g) this region is much wider. Nevertheless, the two different libraries achieve the required representativity value around the same PuO_2 content, i.e., around 22%. The three approaches are summarized in Table 5.

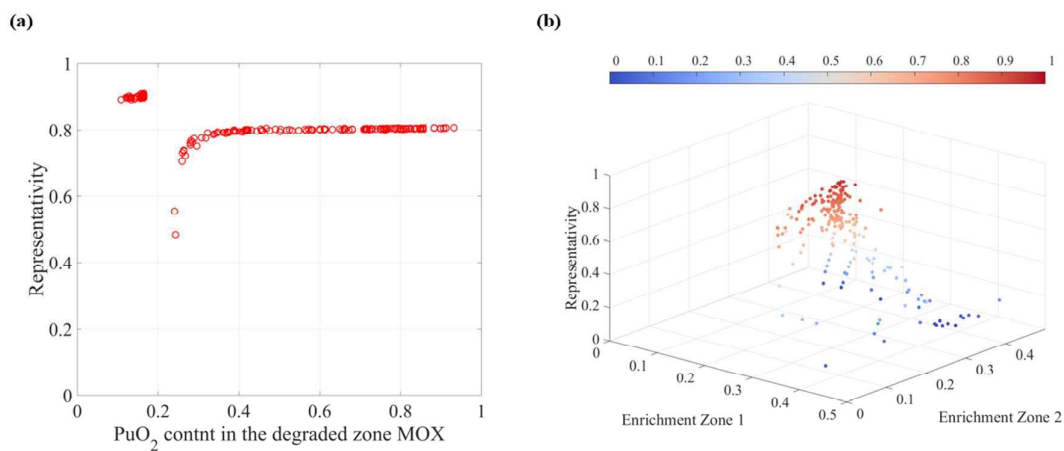


Figure 11: Representativity results of degraded situations using ENDF covariance. (a) Single zone. (b) Two zones.

Table 6: Optimized plutonium content of the ZEPHYR fuel using different ND data.

Covariance data source	Ref. to single deg. zone	r_{RE}	Ref. to two deg. zones		r_{RE}
			Zone 1	Zone 2	
COMAC-V01	22.5%	0.85	20%-24%	20%-24%	0.85-0.87
UCOM-V01AB	25.2%	0.85	22.5%-26.5%	22.5%-26.5%	0.85-0.91
ENDF Covariance	22%	0.96	25%-30%	15%-20%	0.90-0.94

* reference configuration at 900°C.

** degraded configuration at 1000°C.

*** COMAC and UCOM given in 33 energy groups and ENDF in a 175 energy groups.

4. SUMMARY AND CONCLUSIONS

This paper presents the continuous effort put in the design of a novel experimental program related to Gen-IV SCA studies in the future ZEPHYR versatile critical facility to be constructed around 2028 at Cadarache, France. This novel experimental program belongs to a new class of representative experiments, where zero-power critical facilities (e.g., ZEPHYR) are utilized for studying severe core accidents and reactivity effects in power reactors and in high temperatures. This paper summarizes the additional capabilities developed for this experimental program.

This study is a significant augmentation of the previously designed innovative heuristic approach, which is based on coupling Monte Carlo sensitivity calculation with advanced stochastic optimization method. In this study, the modeling capabilities in the ZEPHYR are extended beyond SFR to include also Gen-IV LFR designs.

The capabilities extension to include Gen-IV Lead-cooled Fast Reactors is carried out using the design of the European Lead SYstem (ELSY) serving as a reference system. The study addresses the challenges related to the design of a representative experiment for a single degraded ELSY fuel assembly. Due to the lack of covariance data related to lead in COMAC-V01, the ENDF covariance data was utilized in 175 energy groups.

Considering SCA in ELSY, two configurations are considered as extremes (e.g., Figures 3 and 7). The two degraded configurations represent a meltdown of the MOX fuel and the formation of a molten region with material stratification, without and with lead reflooding of the voided zone above the melted fuel (e.g., Figures 7b and 7c, respectively). The design optimization process reveals that it is possible to identify highly representative configurations, to be loaded into the ZEPHYR core, of the reactivity variation related to ELSY, as shown in Figure 8 and detailed in

Table 4.

The impact of the energy group structure of the covariance data on the representativity process is examined using both JEFF and ENDF evaluations. For this purpose, the representativity of a single degraded ASTRID fuel assembly is revisited. This energy group collapse is shown to induce a profound impact on the value of the representativity factor since some information is bound to vanish during the collapsing process. For example, the correlation between the different energy groups is smoothed out in the JEFF 33g with respect to the ENDF 175g (e.g., Figures A1-A3). It is also shown that not only the maximal representativity value is strongly affected by the energy group structure of the covariance data. The shape of the search space itself, as sampled by the PSO process, is also significantly affected (Figure 11). Finally, it is demonstrated that finer group structure of the covariance data eventually results in better representativity values and more robust design optimization process (Table 6).

By extending the proposed representative experimental program to two Gen-IV systems, the flexibility of the ZEPHYR facility is enhanced such that it can accommodate almost any other Gen-IV system characterized by different fuels and coolants.

The main novelty of the proposed methodology remains the representativity of high-temperature effects, which characterize power systems, and their transfer to density effects in zero-power critical facilities. In this study, this novel methodology is further qualified by applying it to study a single fuel assembly SCA in the ELSY design, and successfully obtaining high representativity values. This study is a necessary preliminary step towards further qualification of the methodology on a full core SCA for both the SFR and LFR cores in the ZEPHYR facility.

5. ACKNOWLEDGMENTS

This R&D work was performed within a scientific collaboration program between CEA Cadarache and Ben-Gurion University of the Negev.

The research was partially funded by the Israeli Ministry of Energy, contract number 215-11-020.

Bibliography

1. International Atomic Energy Agency. *The Fukushima Daiichi accident*. Vienna 2015. GC(59)/14.
2. Sehgal BR, ed. *Nuclear Safety in Light Water Reactors*. 1 ed. Amsterdam: Academic Press; 2012.

- 1
- 2
- 3 3. IAEA. *Safety Reports Series*. Vienna 2008.
- 4 4. IAEA. *Status of Fast Reactor Research and Technology Development*. Vienna: IAEA; 2013.
- 5
- 6 5. Van Dorsseleare JP, Albiol T, Micaelli JC. Research on Severe Accidents in Nuclear Power
- 7 Plants. In: Tsvetkov P, ed. *Nuclear Power - Operation, Safety and Environment*. Rijeka:
- 8 INTECH; 2011.
- 9
- 10 6. GIF. *A Technology Roadmap for Generation IV Nuclear Energy Systems*. Paris: GIF; 2014.
- 11
- 12 7. Margulis M, Blaise P, Gilad E. Modeling Representative Gen-IV Molten Fuel Reactivity
- 13 Effects in the ZEPHYR Fast/Thermal Coupled ZPRs. Part I - Assembly Level. *International*
- 14 *Journal of Energy Research*. April 2018;42(5):1950-1972.
- 15
- 16 8. Dos Santos N, Blaise P, Santamarina A. A global approach of the representativity concept
- 17 Application on a high-conversion sub-moderated MOX lattice case. Paper presented at:
- 18 M&C-2013, 2013; Sun Valley, ID, USA.
- 19
- 20 9. Lebrat JF, Tommasi J. The use of representativity theory in the depletion calculations of SFR
- 21 blankets. *Annals of Nuclear Energy*. 2017;101:429-433.
- 22
- 23 10 Bertrand F, Marie N, Prulhiere G, Lecerf J, Seiler JM. Comparison of the behaviour of two
- 24 core designs for ASTRID in case of severe accidents. *Nuclear Engineering and Design*.
- 25 2016;297:327-342.
- 26
- 27 11 Asahi Shimbun. Scaling back of French reactor a blow for nuke fuel reprocessing. *The Asahi*
- 28 *Shimbun*. May 31, 2018. Available at:
- 29 <http://www.asahi.com/ajw/articles/AJ201805310040.html>. Accessed May 31, 2018.
- 30
- 31 12 Blaise P, Boussard F, Leconte P, et al. Experimental R&D innovation for Gen-II,III & IV
- 32 neutronics studies in ZPRs: a path to the future ZEPHYR facility in Cadarache. Paper
- 33 presented at: IGORR-2016, 2016; Berlin, Germany.
- 34
- 35 13 Alemberti A, Carlsoon J, Malambu E, et al. European lead fast reactor ELSY. *Nuclear*
- 36 *Engineering and Design*. 2011;241(9):3470-3480.
- 37
- 38 14 Orlov VV. Problem of fast reactor physics related to breeding. *Atomic energy review*.
- 39 1980;January:989-1077.
- 40
- 41 15 WNN. Molten salt reactor experiment begins at Petten. *World Nuclear News*. September 06,
- 42 2017. Available at:
- 43 [http://www.world-nuclear-news.org/NN-Molten-salt-reactor-experiment-begins-at-Petten-060](http://www.world-nuclear-news.org/NN-Molten-salt-reactor-experiment-begins-at-Petten-0609174.html)
- 44 [9174.html](http://www.world-nuclear-news.org/NN-Molten-salt-reactor-experiment-begins-at-Petten-0609174.html).
- 45
- 46 16 Ronen Y. *Uncertainty analysis*: CRC Press; 1988.
- 47
- 48
- 49
- 50
- 51
- 52 17 Soppera N, Bossant M, Dupont E. JANIS 4: An Improved Version of the NEA Java-based
- 53 Nuclear Data Information System. *Nuclear Data Sheets*. 2014;120:294-296.
- 54
- 55 18 Aufiero M, Bidaud AV, Hursin M, et al. A collision history-based approach to
- 56
- 57 20 / 23
- 58
- 59
- 60

- 1
2
3 . sensitivity/perturbation calculations in the continues energy Monte Carlo code Serpent.
4 *Annals of Nuclear Energy*. 2015;85:245-258.
5
6 19 Dos Santos N. *Optimisation de l'approche de représentativité et de transposition pour la*
7 *conception neutronique de programmes expérimentaux dans les maquettes critiques*.
8 Grenoble: Universite de Grenoble; 2013.
9
10 20 Chenaud MS, Devictor N, Mignot G, et al. Status of the ASTRID core at the end of the
11 pre-conceptual design phase 1. *Nuclear Engineering and Technology*. 2013;45(6):721-730.
12
13 21 Cacuci DG, ed. *Handbook of Nuclear Engineering*. Vol 1. New York: Springer; 2010.
14
15 .
16 22 Piro IL, ed. *Handbook of Generation IV Nuclear Reactors*. Cambridge: Woodhead Publishing;
17 . 2016.
18
19 23 Aït Abderrahim H. Multi-purpose hYbrid Research Reactor for High-tech Applications a
20 multipurpose fast spectrum research reactor. *International Journal of Energy Research*.
21 December 2012;36(15):1331-1337.
22
23 24 Dragunov YG, Lemekhov VV, Moiseev AV, Smirnov VS. Lead-Cooled Fast-Neutron Reactor
25 (BREST). Paper presented at: 48th Meeting IAEA TWG FR, 2015; Obninsk.
26
27 25 Ponciroli R, Cammi A, Lorenzi S, Luzzi L. A preliminary approach to the ALFRED reactor
28 control strategy. *Progress in Nuclear Energy*. May 2014;73:113-128.
29
30 26 Alemberti A, Carlsoon J, Malambu E, et al. European lead fast reactor—ELSY. *Nuclear*
31 *Engineering and Design*. September 2011;241(9):3470-3480.
32
33 27 Ghasabyan LK. *Use of Serpent Monte-Carlo code for development of 3D full-core models of*
34 *Gen-IV fast-spectrum reactors and preparation of group constants for transient analyses with*
35 *PARCS/TRACE coupled system*. Stockholm: KTH Engineering Sciences; 2013.
36
37 28 Margulis M, Blaise P, Mellier F, Gilad E. The path for innovative severe accident neutronics
38 studies in ZPRs. Part I.2 - Impact of nuclear data uncertainties on reactivity changes of
39 SNEAK-12A core. *Progress in Nuclear Energy*. 2017;96:97-117.
40
41 29 Margulis M, Blaise P, Millier F, Gilad E. The path for innovative severe accident neutronics
42 studies in ZPRs. Part II.2 - Impact of nuclear data uncertainties on reactivity changes of
43 SNEAK-12B core. *Progress in Nuclear Energy*. May 2018;105:124-138.
44
45 30 Margulis M, Blaise P, Gabrielli F, Gruel A, Mellier F, Gilad E. The path for innovative severe
46 accident neutronics studies in ZPRs. Part I.1 - Analysis of SNEAK-12A experiments for core
47 disruption in LMFBRs. *Progress in Nuclear Energy*. 2017;94:106-125.
48
49 31 Margulis M, Blaise P, Gabrielli F, Gruel A, Mellier F, Gilad E. The path for innovative severe
50 accident neutronics studies in ZPRs. Part II.1 - Analysis of SNEAK-12B experiments for core
51 disruption in LMFBRs. *Progress in Nuclear Energy*; Under review.
52
53 32 Kennedy J, Eberhart RC. *Swarm Intelligence*: Morgan Kaufmann; 2001.
54
55
56
57
58
59
60

33 Margulis M, Blaise P, Rimpault G, Gilad E. Interpretation of the SNEAK-12A/B experimental programs on severe core accidents in LMFBRs Some feedback on nuclear data re-assimilation for the prediction of reactivity changes. Paper presented at: ICAPP-2017, 2017; Fukui/Kyoto, Japan.

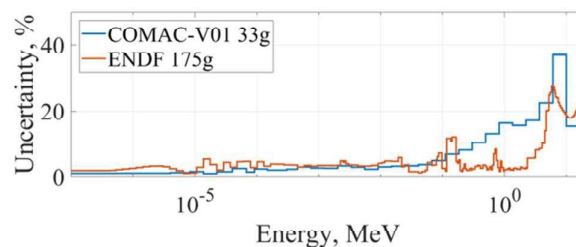
34 Gabrielli F, Rineiski A, Vezzoni B, Maschek W, Fazio C, Salvatores M. ASTRID-like fast reactor cores for burning plutonium and minor actinides. *Ennergy Proccidia*. 2015;71:130-139.

35 Krivitchik G, Blaise P, Coquelet-Pascal C. Artificial neural network surrogate development of equivalence models for nuclear data uncertainty propagation in scenario studies. *EPJ Nuclear Science and Technology*. 2017;3(22):1-15.

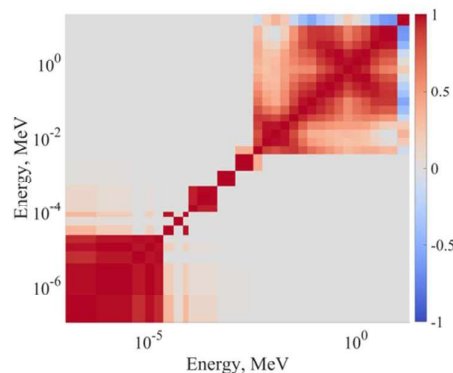
36 Hiruta H, Palmiotti G, Salvatores M, Arcilla Jr. R, Obložinský P, McNight RD. Few Group Collapsing of Covariance Matrix Data Based on a Conservation Principle. *Nuclear Data Sheets*. December 2008;109(12):2801-2806.

A. APPENDIX

(a)



(b)



(c)

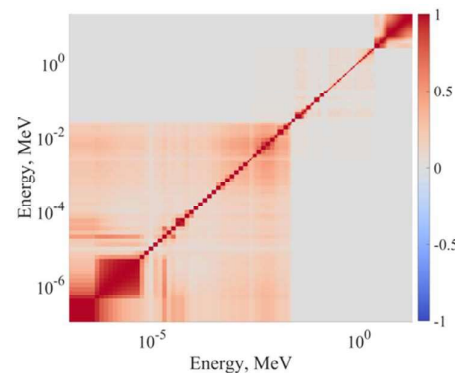


Figure A1: Covariance data for capture of ^{238}U . (a) uncertainty vector comparison (b) COMAC-V01 correlation matrix (c) ENDF correlation matrix.

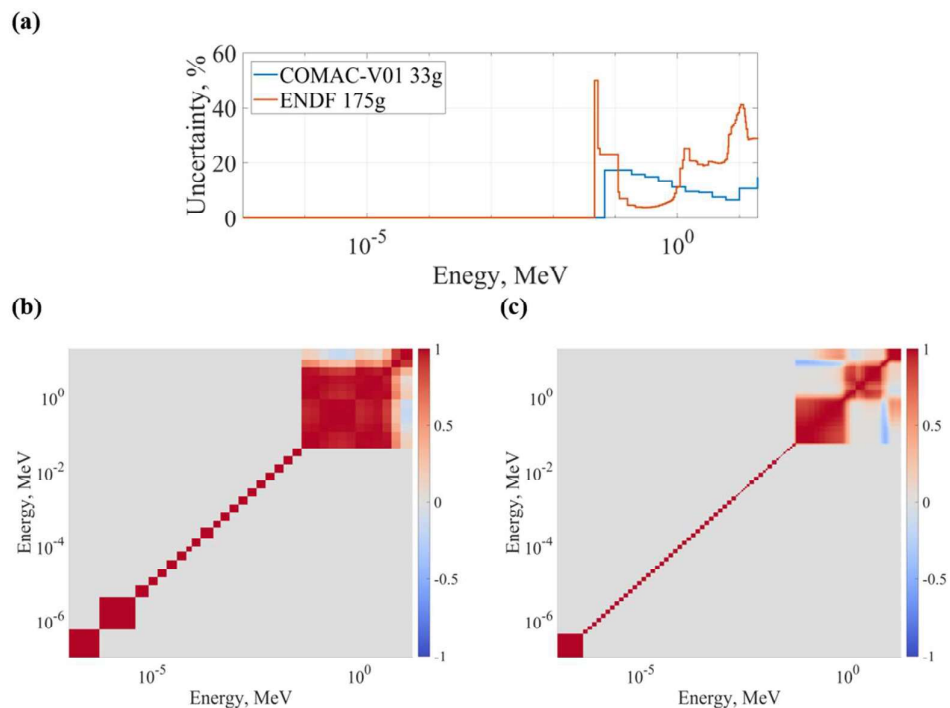


Figure A2: Covariance data for inelastic scattering of ^{238}U . (a) uncertainty vector comparison (b) COMAC-V01 correlation matrix (c) ENDF correlation matrix.

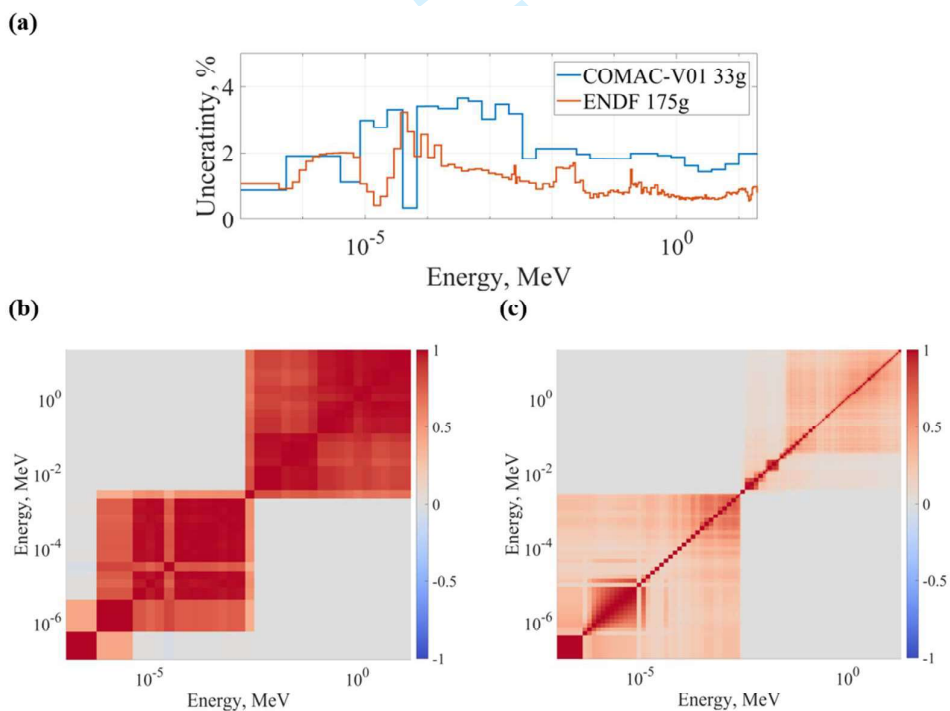


Figure A3: Covariance data for fission of ^{239}Pu . (a) uncertainty vector comparison (b) COMAC-V01 correlation matrix (c) ENDF correlation matrix.